Phase Composition and Microstructure of Zn Coated Press Hardening Steels for Direct Hot Stamping

Vojtěch Kučera[1], Jaroslav Pert-Soini[2], Dalibor Vojtěch[1]
[1]University of Chemistry and Technology, Prague, Department of Metals and Corrosion Engineering, Czech Republic, EU, kucerao@vscht.cz
[2]ŠKODA AUTO a. s., Mladá Boleslav, Czech Republic, EU, jaroslav.petr.soini@skoda-auto.cz

Decarburization and oxidation occur during production of press hardening steels (PHS) used in automotive. Therefore, coatings are applied on the steel surface to prevent this. The most common Zn coatings have not been processable by available direct hot stamping technology ordinarily used to produce the PHS and have been replaced by Al-Si coatings. However, the Al-Si coatings have a negative impact on joining technologies and further processing. Recently, the modification of direct hot stamping, which enables process the PHS with Zn coatings, was introduced. We investigated the microstructure, phase composition and distribution of particular phases (SEM-EDS, XRD), as well as micro-hardness of the Zn coated PHS prepared by the modified direct hot stamping. The PHS revealed the coating with 25 ± 3 µm thickness and continuous interface consisting of α-Fe(Zn) solid solution, Γ and Γ_1 intermetallic phases and zinc oxides enriched with manganese. The thorough description of the material is important in development of further processing steps such as joining technologies and corrosion resistance.

Keywords: Zn coating, press hardening steels, direct hot stamping, liquid metal embrittlement

1 Introduction

There is a constant effort on safetiness and lowering fuel consumption in automotive industry due to CO_2 limits. This leads to the development and utilization of materials with higher strength enabling sheets thinning at the same time. The press hardening steels (PHS) make this goal feasible. They find applications mostly in safety components such as A-pillar, B-pillar, bumper etc. (Fig. 1). Nevertheless, by introducing the PHS into the industry, the issue of the coatings, which provide stable processing and sufficient corrosion protection, is still a big challenge [1-3].

Two methods of processing, which are ordinarily used in the industry, were designed: (i) the direct hot stamping (Fig. 2a) and (ii) the indirect hot stamping (Fig. 2b). During the direct hot stamping (i), the steel sheet is heated up to the austenitizing temperature (~ 900 °C) and subsequently transformed into the water-cooled press, where the sheet is pressed and quenched in single step. The martensitic microstructure reaching strength up to 2000 MPa results from original ferritic/pearlitic steel. However, the PHS suffer from decarburization and oxidation of the surface during the austenitization. Hence, coatings are applied on the steel surface to prevent this. The most common Zn coatings cannot be used due to the high temperatures leading to the liquid metal embrittlement [4, 5]. Therefore, the Zn coatings have been replaced by Al-Si coatings, which provide sufficient protection against oxidation and decarburization during heating and pressing [1]. Although, the microstructure and phase composition of the Al-Si coatings can significantly differ and contain brittle Al-Fe-Si intermetallics. This is caused by high dependence of phase composition on heating conditions. They also do not provide such effective cathodic protection and have worse formability resulting in micro-cracks formation compared to the Zn coatings [6-8]. The indirect hot stamping (ii) involves additional step, cold pressing, which precedes the austenitization. After heating, the steel sheet is then only subjected to quenching and calibration in the press. Although this method allows processing of the PHS with Zn coatings, it is more complicated and expensive [1, 9].

Fig. 1 *Press hardening steels in car body marked with red and orange colour [10].*

Hence, considerable efforts have been devoted to the development of new technologies capable of processing the Zn coatings by the direct hot stamping. T. Kurz et al. [12] reported the modified direct hot stamping, which enables process the Zn coated PHS. The modification of the process eliminates the liquid metal embrittlement leading to the cracking of the coating and steel substrate during the hot stamping. The considerable reduction of micro-cracks due to the decreasing stamping temperature was also observed in [13]. These findings indicate important breakthrough in the field of press hardening steels, and therefore the thorough study of such-prepared PHS is important both in terms of material and coating description, and in terms of further processing.

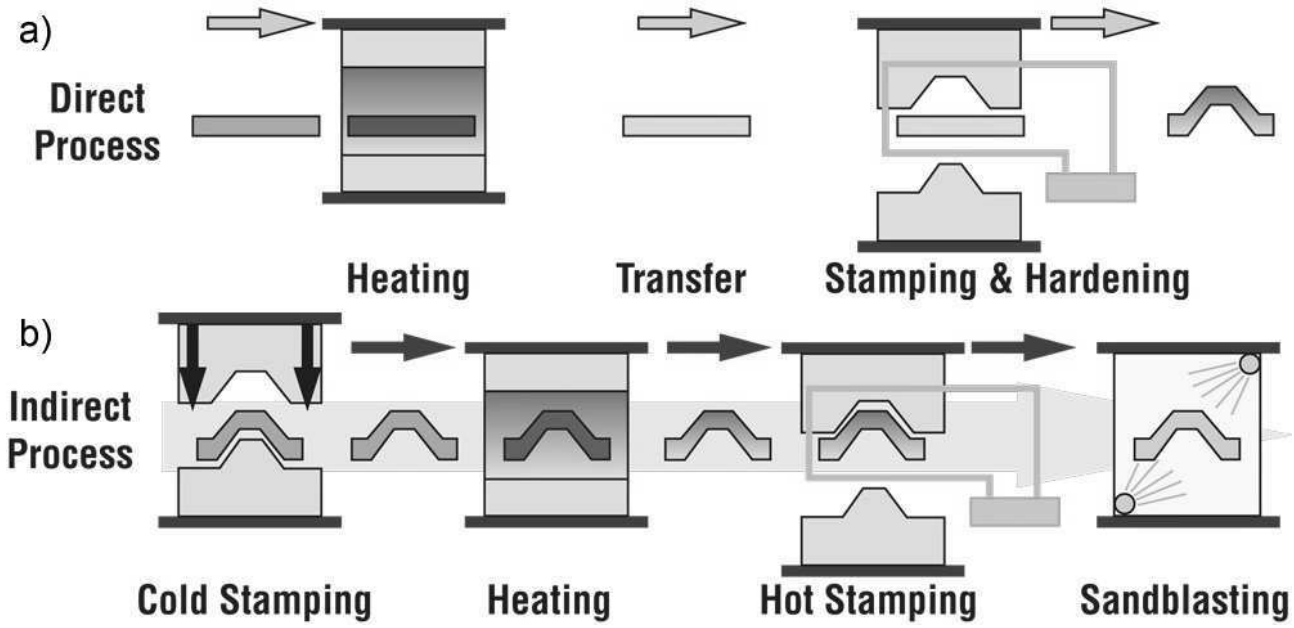

Fig. 2 *The scheme of direct hot stamping a), and indirect hot stamping b) [11].*

In this work, we described the microstructure and phase distribution through the interface between the base material and Zn coating of the PHS steel prepared by the modified direct hot stamping process with incorporated pre-cooling step. We also measured the micro-hardness profile of the coating. In automotive, resistance spot welding is still the most widely used method and the coatings on the steel surface strongly influence the welding parameters [14]. Thus, the characterization of the coating and the coating/substrate interface could provide important findings for further processing.

2 Experiment

The steel sheets with the thickness of 1.5 mm were used in this experiment. The chemical composition of the as-received steel sheet was measured by the optical emission spectrometer (OES) Bruker and is shown in Tab. 1. According to the chemical composition, the steel is manganese-boron steel used for press hardening [15]. The sheets were cut into the samples for metallography observing in the direction of rolling and in the direction perpendicular to the rolling. The samples for microstructure observation were prepared by standard metallography procedure including grinding at SiC papers and polishing using diamond suspensions. Two-step etching [16] was used to reveal the microstructure of the coating and base steel material. The etchant comprises 1 % solution of HNO_3 in amyl alcohol and 1 % solution of picric acid in amyl alcohol with addition of HF. The microstructure was observed by the optical microscope (Olympus GX71) and the scanning electron microscope (Tescan Vega 3 LMU, accelerating voltage 20 kV, detector SE + BSE) equipped with the energy dispersive spectroscopy detector (Oxford Instruments INCA 350, 20 mm^2). The X-ray diffraction data were collected at room temperature with a Bruker AXS D8 θ-θ powder diffractometer with parafocusing Bragg-Brentano geometry using CoK_α radiation (λ = 1.79021 Å, U = 34kV, I = 20 or 30 mA). Data were scanned with an ultrafast detector LynxEye over the angular range 5-60° (2θ) with a step size of 0.0196° (2θ) and a counting time of 19.2 s $step^{-1}$. Data evaluation were performed in the software package HighScore Plus 3.0e. The micro-hardness was measured by Vickers (Future Tech FM-700) with the load of 5 g and with the step of 20 μm between the two adjacent indentations.

Tab. 1 *The chemical composition of the PHS without Zn coating measured by OES in wt. %.*

Element	C	Si	Mn	P	S	Al	Cr	Ti	B
wt. %	0.18	0.17	1.97	0.011	0.0008	0.039	0.026	0.03	0.002

3 Results and discussion

The modified direct hot stamping for the Zn coated PHS introduces the material with specific Zn coating composition and Zn/Fe interface. The X-ray diffraction analysis (Fig. 3) revealed binary Zn-Fe intermetallic phases. These intermetallics were determined as Γ and Γ_1. The Γ phase is predominantly referred to Fe_3Zn_{10}, although can be also described as Fe_4Zn_9 or $FeZn_3$ due to the variable Fe content. It crystallizes by the peritectic reaction between α-Fe and Zn-rich liquid at 782 °C in the body centred cubic structure with the Fe content in the range of 23.5–28 wt.%. The Γ_1 is expressed by stoichiometric formula Fe_5Zn_{21} or $Zn_{11}Zn_{40}$ and it has face centred cubic crystalline lattice consisting 17-19.5 wt. % Fe. It forms by the peritectoid reaction between the Γ phase and the δ phase at approximately 550 °C [17, 18]. This suggests that the δ phase is present at higher temperatures,

but it is consumed by peritectoid reaction. Those two intermetallic phases (Γ, $Γ_1$) are the richest in iron content, which indicates significant diffusion between the base martensitic steel and Zn coating. The XRD also showed presence of zinc oxide, which was attributed to the surface oxidation. The XRD pattern was compared with base martensitic steel without Zn coating. Three peaks corresponding to iron are clearly visible. The peak intensity of Fe at the Zn coated PHS was relatively weak, because the X-ray radiation probably did not penetrate into the base material. The penetration is dependent on the absorption of the Zn coating phases and was not studied in this experiment.

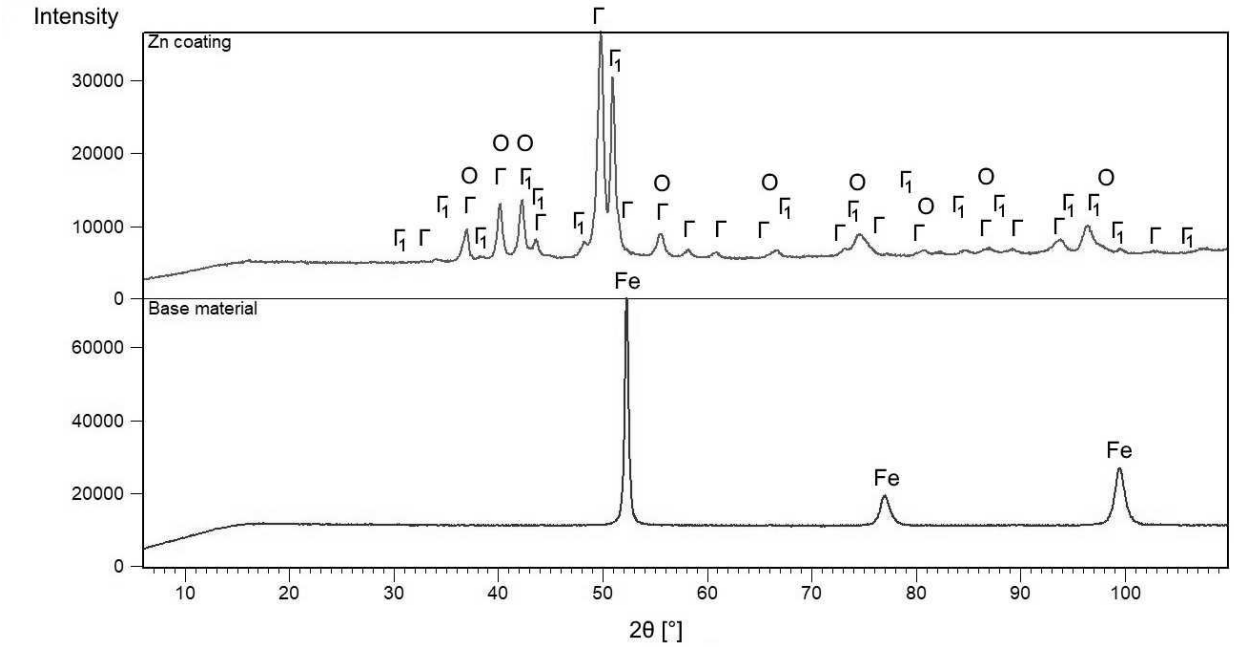

Fig. 3 *The X-ray diffraction phase analysis of Zn coating and base material without coating. (Γ-gamma phase, $Γ_1$ - gamma1 phase, O – oxide, Fe – iron)*

The SEM image (Fig. 4) revealed Zn layer with the average thickness of 25 ± 3 µm. The etching was performed by two-step etching in 1 % solution of HNO_3 in amyl alcohol and 1 % solution of picric acid in amyl alcohol with the addition of HF. The amyl alcohol slowly attacks the microstructure and thus was used instead of ethanol to better control the etching. The microstructure of Zn coating and base material is shown in Fig. 4a. The coating was formed mostly by the relatively large grains and top-surface layer. The areas with the dark grey colour corresponded to the Fe-rich regions and the top-surface (light grey) coating layer to the Zn-rich regions and probably some oxides. The microstructure of base material (Fig. 4b) was composed of lath martensite, which forms during press hardening from originally ferritic/pearlitic steel.

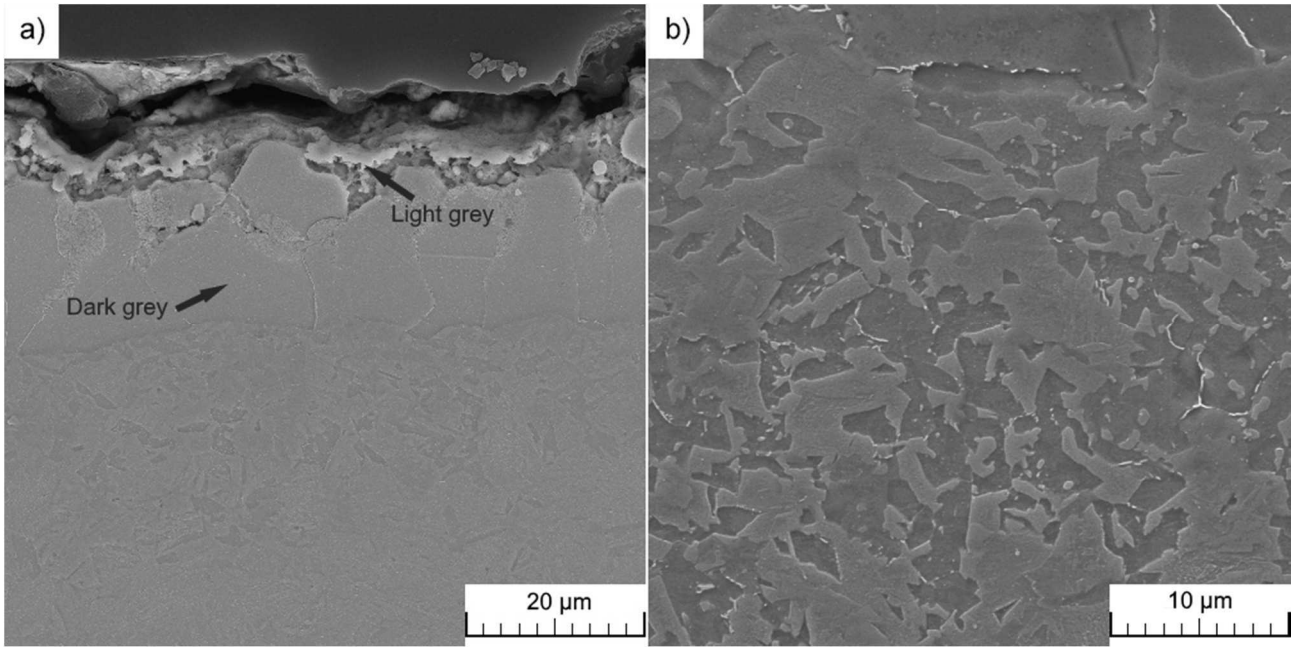

Fig. 4 *The SEM image of Zn coating microstructure (a) and base material (b).*

To more accurate description and distribution of the phases in the Zn coating, the oblique cut was analysed by BSE and EDS point analysis of chemical composition (Fig. 5). The Zn-rich areas (light grey) can be clearly distinguished and they concentrated in the top-surface layer, while the Fe-rich regions (dark grey) were located near the Zn-coating/Fe substrate interface. The isolated dark grey areas were also observed in the top-surface layer of the coating (see in detail in Fig. 5b). The EDS analysis was performed to identify the particular phases and the results are summarized in Tab. 2. The isolated dark grey areas in the top-surface layer were connected to the surface oxidation and corresponded to zinc/iron oxides (Fig. 5b, point 1) and to zinc/iron oxides enriched with manganese (Fig. 5b, point 2). Manganese has higher affinity to oxygen than Fe and probably diffused from the base material at elevated temperatures during the austenitization period to formed mixed oxides with Zn and Fe. The Zn-rich phases (light grey) had Fe content in the range from 13.3 to 16.5 wt. % and 22.0–27.2 wt. %. These phases were determined in respect to the literature and binary phase diagram [17, 18] as Γ_1 (Fig. 5b, point 4) and Γ (Fig. 5b, c, point 3,6), respectively. The phase near the coating/substrate interface was rich in Fe (dark grey) and contained 62.5–68.5 wt. % of Fe (Fig. 5c, point 7), where the Fe content increased into the substrate until 86.2 wt. % following the diffusion path (Fig. 5a, point 9). This phase was identified as α-Fe. The maximum solubility of Zn in α-Fe solid solution is approximately 46 wt. % at 782 °C [18]. The rapid quenching during press hardening could lead to the forming of the supersaturated solid solution and thus increase Zn content. The regions adjacent to the grain boundaries in the coating depicted in Fig. 5c (point 8) had 71–76 wt. % of Fe and were also identified as α-Fe. During the austenitization at approximately 900 °C, the strong diffusion and enrichment of Zn coating by Fe can be expected. At this temperature, only α-Fe is solid and coexists with Zn-rich liquid. According to the phase diagram, the Γ phase solidifies at ~782 °C by the peritectic reaction and Γ_1 at ~550 °C the peritectoid reaction, respectively. These two-phase transformations should occur before press hardening to prevent the presence of the Zn-rich melt causing the liquid metal embrittlement.

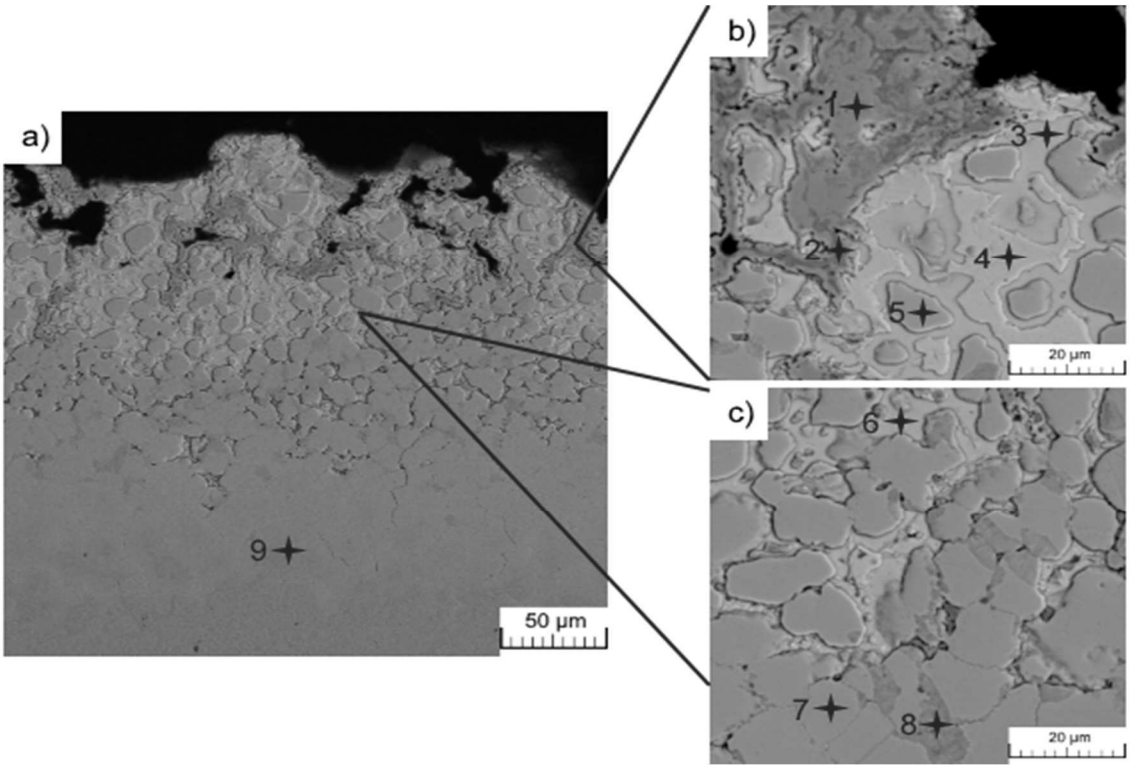

Fig. 5 *The SEM-BSE image and EDS chemical point analyses of Zn coating.*

Tab. 2 *The results from SEM-EDS chemical point analysis of Zn coating in wt. %.*

Point	O	Mn	Fe	Zn	Phase
1	10.4	0.3	5.4	83.9	Zn, Fe oxide
2	13.7	25.6	4.3	56.4	Zn, Mn, Fe, oxide
3			25.4	74.6	Γ
4			15.8	84.2	Γ_1
5			63.2	36.8	α-Fe
6			25.3	74.7	Γ
7			66.9	33.1	α-Fe
8			72.8	27.2	α-Fe
9		1.3	86.2	12.5	α-Fe

The micro-hardness profile depending on distance from the surface into the base material is shown in Fig. 6. Initially, the micro-hardness decreased from approximately 300 HV to 275 HV into the coating/substrate interface and then increased again up to 373 HV. The Zn-Fe intermetallic phases, which develop during hot dip galvanizing, are reported to be hard and brittle [19]. In [18] stated that the Γ_1 phase had the highest measured micro-hardness. Hence, the Γ_1, Γ phases could contribute to the relatively high micro-hardness of the top-surface layer. The decrease of the micro-hardness into the coating/substrate interface could be attributed to the layer of α-Fe

solid solution supersaturated by Zn forming during austenitization and rapid quenching by the press hardening. Further increase related to the exceeding the coating/substrate interface to the base material. The micro-hardness of the base material was 359 ± 14 HV.

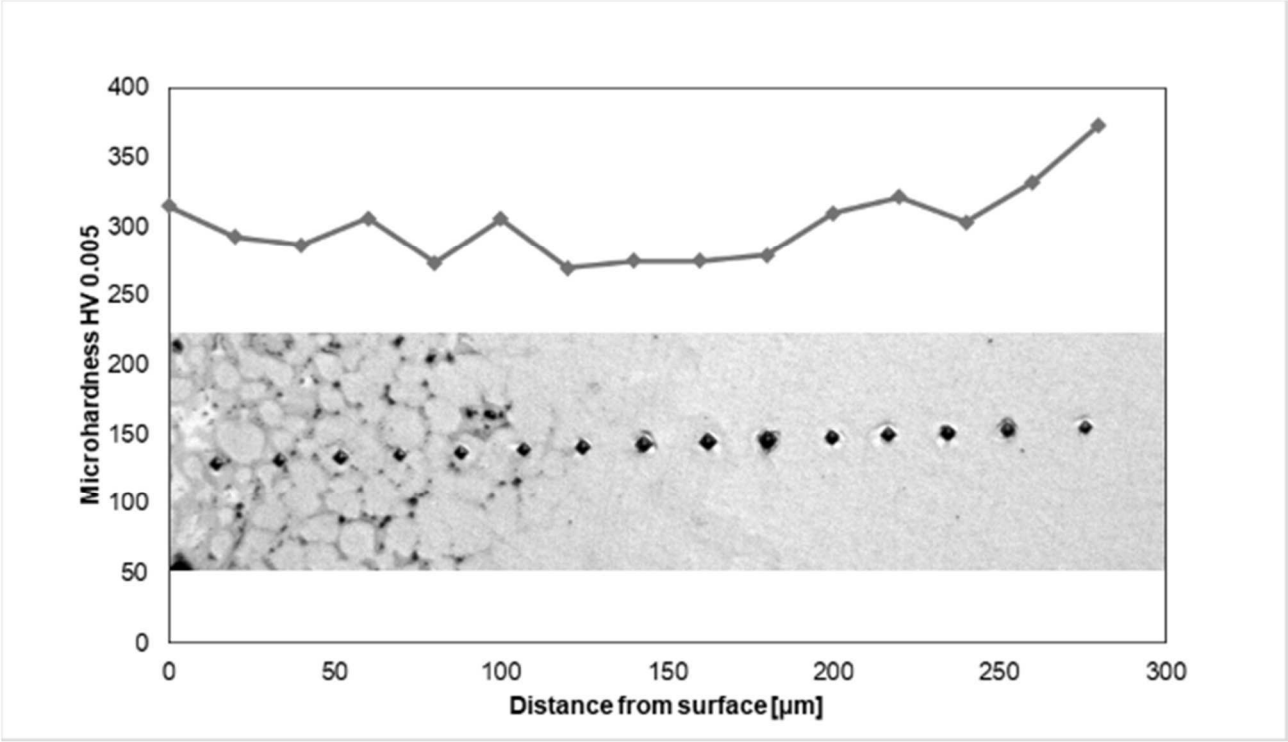

Fig. 6 *The micro-hardness profile of the coating measured by Vickers with the load of 5 g.*

4 Conclusion

In most cases, the Al-Si coated press hardening steels produced by direct hot stamping are used in car body manufacturing. However, the modification of direct hot stamping method enables to process Zn coated steels and introduces the important breakthrough in the field of the press hardening steels. Such Zn coated PHS was investigated in this study in terms of the microstructure and phase composition. The Zn coating had the thickness of 25 ± 3 µm and its micro-hardness decreased into to the coating/substrate interface. Most of the coating was comprised of α-Fe solid solution with the top-surface layer forming by Zn-rich phases Γ_1 and Γ, respectively, and oxides. The coatings and its phase composition strongly affect further processing steps, especially the joining, and thus its thorough characterization provide important findings in further research.

Acknowledgement

The authors wish to thank the Financial support from specific university research (MSMT No 21-SVV/2018) for its financial support of this research.

References

[1] H. KARBASIAN, A.E. TEKKAYA. (2010). A review on hot stamping. In: *Journal of Materials Processing Technology*, Vol. 210, No. 15, pp. 2103-2118

[2] V.H. LÓPEZ-CORTÉZ, F.A. REYES-VALDÉS. (2008). *Understanding Resistance Spot Welding of Advanced High-Strength Steels*, 36-40.

[3] P. HANUS, E. SCHMIDOVÁ. (2016). Influence of the welding process on the martensitic and dual phase high strength steels. In: *Manufacturing Technology*, Vol. 16, No. 4, pp. 702-707

[4] J. MENDALA. (2012). Liquid metal embrittlement of steel with galvanized coatings. In: *IOP Conf. Series: Materials Science and Engineering*, Vol. 35, No., pp. 1 - 8

[5] L. CHO, et al. (2014). Microstructure of liquid metal embrittlement cracks on Zn-coated 22MnB5 press-hardened steel. In: *Scripta Materialia*, Vol. 90-91, No., pp. 25-28

[6] Z.-X. GUI, W.-K. LIANG, Y.-S. ZHANG. (2014). Formability of aluminum-silicon coated boron steel in hot stamping process. In: *Transactions of Nonferrous Metals Society of China*, Vol. 24, No. 6, pp. 1750-1757

[7] C. KIM, M.J. KANG, Y.D. PARK. (2011). Laser welding of Al-Si coated hot stamping steel. In: *Procedia Engineering*, Vol. 10, No., pp. 2226-2231

[8] Z. GUI, W. LIANG, Y. ZHANG. (2014). Enhancing ductility of the Al-Si coating on hot stamping

steel by controlling the Fe-Al phase transformation during austenitization. In: *Science China Technological Sciences*, Vol. 57, No. 9, pp. 1785-1793

[9] H. PING, Y. LIANG, H. BIN. (2017). *Hot Stamping Advanced Manufacturing Technology of Lightweight Car Body*, XVI, 314. Springer Singapore.

[10] W. STEED. *Hot off the press*. 2014 [cited 2018 18.06.]; Available from: https://automotivemanufacturingsolutions.com/technology/hot-off-the-press.

[11] E.F. WILLIAM. *New coil-applied nonmetallic coating protects press-hardenable steel*. 2015 [cited 2018 29.05.]; Available from: https://www.thefabricator.com/article/metalsmaterials/new-coil-applied-nonmetallic-coating-protects-press-hardenable-steel.

[12] T. KURZ, et al. (2016). Press-hardening of zinc coated steel - characterization of a new material for a new process. In: *IOP Conference Series: Materials Science and Engineering*, Vol. 159, No. 1, pp. 012025

[13] G. HENSEN, et al., Unlocking the potential of zinc coated steel for hot forming by innovative process modifications, in *CHS2 2015, 5th International Conference on Hot Sheet Metal Forming of High-Performance Steel*. 2015, erlag Wissenschaftliche Scripten: Toronto. p. 85-92.

[14] Y.K. BUDIONO, S.Y. MARTOWIBOWO. (2017). Optimization of Resistance Spot Welding process using Response Surface Methodology and Simulated Annealing. In: *Manufacturing Technology*, Vol. 17, No. 4, pp. 434-440

[15] H. JIRKOVÁ, et al. (2018). Use of the press hardening technology for treatment of TRIP steel. In: *Manufacturing Technology*, Vol. 18, No. 2, pp. 243-247

[16] C.E. JORDAN, et al. (1993). Metallographic preparation technique for hot-dip galvanized and galvannealed coatings on steel. In: *Materials Characterization*, Vol. 31, No. 2, pp. 107-114

[17] P. POKORNY, et al. (2015). Description of structure of Fe-Zn intermetalic compounds present in hot-dip galvanized coatings on steel. In: *Metalurgija*, Vol. 54, No. 4, pp. 707-710

[18] A.R. MARDER. (2000). The metallurgy of zinc-coated steel. In: *Progress in Materials Science*, Vol. 45, No. 3, pp. 191-271

J.D. CULCASI, et al. (1999). Control of the growth of zinc–iron phases in the hot-dip galvanizing process. In: *Surface and Coatings Technology*, Vol. 122, No. 1, pp. 21-23

10.21062/ujep/173.2018/a/1213-2489/MT/18/5/758